

The Influence of Femoral Internal and External Rotation on Cartilage Stresses within the Patellofemoral Joint

Thor F. Besier,¹ Garry E. Gold,² Scott L. Delp,^{1,3,4} Michael Fredericson,¹ Gary S. Beaupré⁴

¹Department of Orthopedics, Sports Medicine Center, Arrillaga Recreation Center, 341 Galvez Street, Stanford University, Stanford, California 94305-6175, ²Department of Radiology, Stanford University Medical Center, Stanford, California, ³Department of Bioengineering, Stanford University, Stanford, California, ⁴VA Rehabilitation Research and Development Center, Palo Alto, California

Received 13 March 2007; accepted 11 February 2008

Published online 3 June 2008 in Wiley InterScience (www.interscience.wiley.com). DOI 10.1002/jor.20663

ABSTRACT: Internal and external rotation of the femur plays an important role in defining the orientation of the patellofemoral joint, influencing contact areas, pressures, and cartilage stress distributions. The purpose of this study was to determine the influence of femoral internal and external rotation on stresses in the patellofemoral cartilage. We constructed finite element models of the patellofemoral joint using magnetic resonance (MR) images from 16 volunteers (8 male and 8 female). Subjects performed an upright weight-bearing squat with the knee at 60° of flexion inside an open-MR scanner and in a gait laboratory. Quadriceps muscle forces were estimated for each subject using an electromyographic-driven model and input to a finite element analysis. Hydrostatic and octahedral shear stresses within the cartilage were modeled with the tibiofemoral joint in a “neutral” position and also with the femur rotated internally or externally by 5° increments to ±15°. Cartilage stresses were more sensitive to external rotation of the femur, compared with internal rotation, with large variation across subjects. Peak patellar shear stresses increased more than 10% with 15° of external rotation in 75% of the subjects. Shear stresses were higher in the patellar cartilage compared to the femoral cartilage and patellar cartilage stresses were more sensitive to femoral rotation compared with femoral cartilage stress. Large variation in the cartilage stress response between individuals reflects the complex nature of the extensor mechanism and has clinical relevance when considering treatment strategies designed to reduce cartilage stresses by altering femoral internal and external rotation. © 2008 Orthopaedic Research Society. Published by Wiley Periodicals, Inc. *J Orthop Res* 26:1627–1635, 2008

Keywords: femur rotation; cartilage stress; patellofemoral joint

Articular cartilage plays an integral role in the distribution of joint loads to underlying bone, and displays unique mechanical properties that allow it to sustain considerable repetitive loads. This is particularly important at the patellofemoral joint, which experiences contact forces greater than body weight (BW) during everyday activities such as walking (~1.2 × BW),¹ climbing stairs (3.0 to 3.5 × BW),^{2,3} or running (7.0 to 11.0 × BW).⁴ Any change in the mechanical environment, via altered joint kinematics or load distribution, will affect the stress state of the cartilage, subchondral bone, and cancellous bone, ultimately influencing the physiology and morphology of the joint.

Altered stresses in the cartilage may also play a role in a pain response, by transferring stresses into the underlying subchondral bone and exciting nociceptors. Increased cartilage and subchondral bone stress has been postulated as a mechanical etiology for patellofemoral pain⁵ and has been supported, in part, by estimates of average joint stresses (force/area) in patients with patellofemoral pain.⁶ Although several researchers have measured and modeled contact pressures at the patellofemoral joint,^{6–10} cartilage contact pressures alone do not represent the stresses within the tissue, in particular, the shear stresses,¹¹ which are believed to be important for cartilage degeneration.¹² Estimating in vivo stresses throughout articular cartilage is challenging, and may be influenced by factors

such as joint geometry, cartilage morphology, and material properties, muscle forces, and the orientation of the articulating bodies. One goal of this work is to use subject-specific finite element models to estimate cartilage stresses in both the femur and the patella in a range of subjects and determine the sensitivity of cartilage stress to changes in femoral orientations.

Of particular interest to the clinical community is the potential of femoral internal and external rotation to influence stresses at the patellofemoral joint. During active knee flexion, the femur typically undergoes external rotation with respect to the tibia. Kinematic studies using bone pins^{13,14} or imaging techniques^{15,16} have shown the femur to rotate with respect to the tibia as much as 10° during the stance phase of gait^{13,14} and up to 20° during a squat to 60° of knee flexion.¹⁵ Powers and colleagues¹⁶ found that under weight-bearing conditions, patients who experienced lateral subluxation of the patella underwent greater hip internal rotation when rising from a squat compared to nonweight-bearing conditions. Internal rotation of the femur^{16–19} has been cited as having an influence on the alignment of the patella, the stresses within the patellofemoral joint, and/or the onset of patellofemoral pain. Lee and colleagues⁹ illustrated how internal rotation of the femur can increase the contact pressures on the lateral facet of the patella, whereas external rotation increased contact pressures on the medial facet. Lee et al.⁸ have also shown that a fixed femoral rotation of the femur can lead to nonlinear increases in the patellofemoral contact pressures, with small increases in pressure from 0 to 20° of internal rotation and much greater increases in pressure from 20 to 30° of rotation. It is not known what effect

Correspondence to: Thor F. Besier (T: 650-736-9855; F: 650-725-2607; E-mail: besier@stanford.edu)

© 2008 Orthopaedic Research Society. Published by Wiley Periodicals, Inc.

these isolated femoral rotations and changes in contact pressures might have on the stresses throughout the cartilage in the femur and patella.

The purpose of this study was to determine the influence of femoral rotation on hydrostatic pressure and octahedral shear stress within the patellofemoral joint cartilage. These two stress invariants were chosen based on previous studies that suggest that these stress measures may play unique and important roles in cartilage mechanobiology.^{12,20} We therefore performed a modeling study and hypothesized that hydrostatic pressure and octahedral shear stresses within the patellofemoral joint cartilage would increase with internal rotation of the femur. Conversely, we hypothesized that patellofemoral joint cartilage stresses would be reduced with femoral external rotation.

MATERIALS AND METHODS

We simulated the patellofemoral joint mechanics during a static squat at 60° of knee flexion. This task involved relative large loads at the patellofemoral joint and was reproducible in both a motion capture laboratory and within an open magnetic resonance imaging (MRI) scanner, facilitating comparison between simulations and experiments. This posture is typical of the knee flexion angle when the largest moments are applied to the knee during stair climbing.³ Squatting is also a task that is often regarded as painful for patients with patellofemoral pain, and has been shown previously to involve substantial femoral rotation.¹⁵

Sixteen subject-specific finite element models of the patellofemoral joint were created. Experimental data were obtained from physically active, pain-free volunteers, including eight females (age: 29 ± 5 years, height: 1.65 ± 0.05 m, mass: 57.4 ± 5.1 kg) and eight males (age: 29 ± 6 years, height: 1.77 ± 0.06 m, mass: 72.6 ± 6.0 kg). Prior to data collection, subjects were informed of all experimental procedures and signed a consent form to comply with the Institutional Review Board of Stanford University.

To define the geometry of the bones and cartilage of the patellofemoral joint, MR images of each subject's knee were acquired with a 1.5T GE Signa MR scanner (GE Healthcare, Milwaukee, WI) using a fat-suppressed spoiled gradient echo sequence (repetition time: 60 ms, echo time: 5 ms, flip angle: 40°, matrix: 256 × 256, field of view: 12 × 12 cm, slice thickness: 1.5 mm, scan time 10:25 min). These high resolution images were manually segmented to create a finite element mesh of the bones of the femur, tibia, and patella, as well as the anterior femoral cartilage and patellar cartilage (Fig. 1a; see ref. 21 for more details).

Each subject was also scanned in an open-configuration MR scanner (0.5T SP/i MR, GE Healthcare, Milwaukee, WI) in an upright, weight-bearing posture with the knee at 60° of knee flexion. A 3D fast spoiled gradient echo sequence was used to obtain contiguous sagittal plane images of the patellofemoral joint (repetition time: 33 ms, echo time: 9 ms, flip angle: 45°, matrix: 256 × 160, field of view: 20 × 20 cm, slice thickness: 2 mm, scan time 2:10 min). These scans were used to register the finite element meshes of the femur, tibia, and patella into the initial configuration for the simulations, as well as to describe the orientation and position of the patellar tendon and quadriceps muscles. An iterative closest point algorithm was

used within custom Matlab software (Mathworks, Natick, MA) selecting at least 30 points on the bone surface to ensure an adequate visual registration between the FE mesh and the volumetric data set. The weight-bearing MR images were also used to measure patellofemoral joint contact areas for each subject, to facilitate model validation.²¹ The estimation of patellofemoral joint contact area has been validated and described previously.^{22,23} The bones of the femur, tibia, and patella were treated as rigid bodies to reduce the computational complexity of the simulation. Because subchondral bone is at least two orders of magnitude stiffer than cartilage,²⁰ treating the subchondral bone as rigid is a reasonable approximation without influencing the stress distribution in the cartilage.^{11,24} The femoral and patellar cartilage was modeled as a linear elastic solid²⁵ with an elastic modulus of 7 MPa and a Poisson ratio of 0.47.²⁶ The nodes of cartilage closest to the bone were connected to the rigid bone elements using a "tied" constraint in ABAQUS (Simulia, Providence, RI). The interaction between the patellar and femoral surfaces was resolved using surface-to-surface contact with a friction coefficient of 0.02.²⁷

The patellar tendon and quadriceps muscles were modeled as tension-only connector elements (Fig. 1a). The patellar tendon was modeled using nine connector elements in a 3 × 3 grid with the relative attachment points chosen to evenly distribute the elements across the attachment area of the tibia and inferior patellar pole. The origin and insertion of the patellar tendon and the insertion of the quadriceps tendon were clearly visible from the MR images. Because the origin of the quadriceps muscle was not visible from the MR images, we estimated the quadriceps line of action by segmenting the

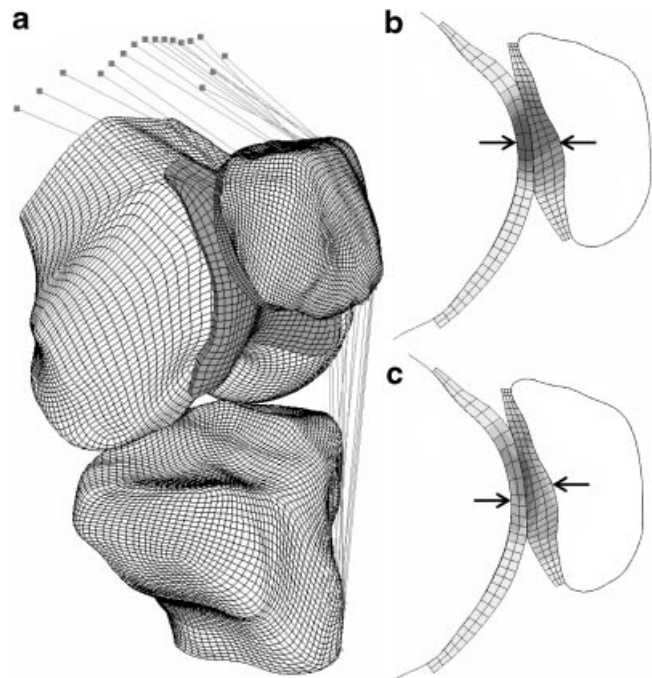


Figure 1. Finite element mesh of the patellofemoral joint (a) illustrating the quadriceps and patellar tendon connector elements. The bone is represented as rigid shell elements, and the cartilage of the femur and patella are deformable hexahedral elements. A sagittal cross-section through the joint shows the distribution of hydrostatic pressure (b) and octahedral shear stress (c) within the femoral and patellar cartilage. Peak and mean cartilage stresses are taken from the layer of elements closest to the bone, as indicated by the arrows.

anterior and inferior aspects of the muscle belly through each MR slice to represent the boundary of the quadriceps muscle and distal tendon insertion. Connector elements were then distributed equally across these segmented surfaces to represent functional components of the quadriceps that could be actuated independently and represented the line of action of each muscle. These functional groups included: the vastus intermedius (two elements), rectus femoris (three elements), vastus lateralis (three elements), vastus lateralis oblique (three elements), vastus medialis (three elements), and vastus medialis oblique (three elements). The origins of these connector elements did not change with the femoral rotation simulations. Nonlinear tendon stiffness was not modeled in these simulations, as the initial orientation of the patella from the weight-bearing MR images represented the patellar tendon under substantial tension. This was considered reasonable, as beyond 30° of knee flexion the patellar tendon does not undergo any significant change in length during weight-bearing flexion.²⁸ Therefore, a linear stiffness of 2000 N/mm in the patellar tendon was used,²⁹ to ensure the patellar did not translate superiorly from its initial configuration based on the MR scan.

Quadriceps, hamstring, and gastrocnemii muscle forces were determined using an electromyographic (EMG) driven musculoskeletal model, using raw EMG and lower limb joint kinematics as input into a modified Hill-type muscle model to calculate muscle forces and net joint moments at the knee.³⁰ Standard stereophotogrammetry techniques were used (Orthotrak, Motion Analysis Corporation, Santa Rosa, CA) to calculate the joint kinematics and kinetics necessary to estimate the muscle forces. Muscle activity was estimated using surface EMG electrodes (MotionLab Systems, Baton Rouge, LA) placed on the following seven muscles crossing the knee: vastus medialis, vastus lateralis, rectus femoris, semimembranosus, biceps femoris, medial gastrocnemius, and lateral gastrocnemius. The anatomical model used for the muscle force predictions treated the vastus medialis and vastus medialis oblique muscles as a single muscle group. Similarly, the representation of the vastus lateralis in the musculoskeletal model included the oblique fibers of this muscle. In the finite element simulation, a percentage of muscle force in the vastus medialis and vastus lateralis muscles were redistributed to oblique fibers of these muscles. These distributions were based on the work of Farahmand et al.,³¹ who showed that the vastus medialis oblique fibers accounted for ~40% of the total muscle physiological cross sectional area of the vastus medialis, and that the vastus lateralis oblique muscles accounted for ~25% of the total cross sectional area of the vastus lateralis. To calibrate the EMG driven model, subjects performed several tasks in a motion capture laboratory including walking, jogging, stair climbing, and single and double leg squatting. The weight-bearing squat performed in the MR scanner was also reproduced in the motion capture laboratory using the same backrest, foot placement, and knee joint angle. This enabled us to estimate the subject-specific muscle forces required to maintain the knee joint at 60° of flexion, including the contribution from the quadriceps, hamstring, and gastrocnemii muscles. It was assumed that the muscle forces obtained in the laboratory represented the muscle forces used to maintain the same position within the open MR scanner. Although the EMG-driven model estimated muscle forces for the hamstring and gastrocnemii muscles, only the quadriceps muscle forces were required as input for the finite element model.

Quasi-static, finite-sliding simulations were performed using a nonlinear FE solver (ABAQUS Standard; Simulia). During each simulation, the femur and tibia were fixed and the patella was allowed to move with 6 degrees of freedom. Quadriceps muscle forces were taken from the EMG-driven model and applied to the patella such that the patella settled into the trochlear groove of the femur, reaching static equilibrium. The initial position or *neutral pose* of the femur and tibia were determined by registering the FE meshes of the femur and tibia to the weight-bearing MR data set. The initial orientation of the patella was also determined by registration to the weight-bearing images. However, to ensure that no overlap existed between the cartilage of the patella and femur, the patella was displaced in an anterior direction until a gap was present between the femoral and patellar cartilage. In subsequent simulations, the femur was rotated about its long axis by 5° increments to a range of ±15°, resulting in seven simulations per subject (112 simulations in total). To ensure the same initial gap between the femur and patella cartilage, the initial orientation of the patella was rotated by the same amount as the femur.

Mean and peak hydrostatic and octahedral shear stresses were calculated from the elements of cartilage closest to the layer of bone (Fig. 1b and c) for each simulation. As a partial validation of each model, the estimated contact area from the simulation was compared to the contact area measured from the weight-bearing MRI. Contact areas were qualitatively compared with the simulations by evaluating the contours of the contact patches. The final orientation of the patella in the simulation was also compared to the orientation of the patella measured from the MR scan, as the simulation in the neutral pose should match the imaging data set. These validations could only be performed for the neutral pose, in which we had obtained the MR images.

It was also of interest to determine how the hydrostatic pressure and octahedral shear stress correlated with the patellofemoral joint contact area and a simplified calculation of the joint stress predicted by the model (force/area). To achieve this, the hydrostatic pressure and octahedral shear stresses were compared with the contact area and the net joint stress (joint reaction force/contact area) obtained from each simulation. Linear, logarithmic, and power curves were used to obtain the best fit to the stress–contact area data, and a linear regression was used to compare the cartilage stress variables with the simplified joint stress. Mean and peak stress variables from the neutral orientation simulations were also compared to a simple measure of joint stress obtained from the estimated joint reaction force and measured joint contact area. Because MR images were only taken in the neutral pose, this comparison was only made for this condition.

To test the hypotheses that cartilage stresses were altered with femoral internal/external rotation, the mean and peak stresses from each simulation were compared to the stresses from the neutral position using a two-factor repeated measures ANOVA [femoral rotation × cartilage site (femur or patella)], with significance set at $p < 0.05$. This analysis also enabled a comparison of mean and peak stresses between the femur and the patellar cartilage at each femur orientation. To account for large variation in stress responses between individuals, subjects were also grouped into categories, based on whether a stress variable “increased” more than 10% or “decreased” more than 10% with a 15° rotation of the femur, compared to the neutral position. If the stress variable remained within ±10% of the stress estimated at the neutral position with a 15° rotation

of the femur then a condition of “no change” was defined. Based on previous measurements of femoral internal/external rotation during a weight-bearing squat or running task,^{13,15,16} 15° was considered to be a maximum physiological range of motion that might occur during a functional task, such as running and cutting.

RESULTS

Muscle Force Distributions

To sustain a double-leg static squat with the knee at 60° flexion, the EMG-driven model predicted mean, net quadriceps forces of 1174 ± 165 N for all subjects. The range of quadriceps loads was 845 N (56.4 kg female) to 1503 N (76 kg male). The average (±SD) distribution of force among the quadriceps muscles were as follows: Rectus femoris 5 ± 3%; Vastus medialis 22 ± 6%; Vastus intermedius 28 ± 2%; Vastus lateralis 44 ± 7%. These muscle forces resulted in a net joint reaction force of 1184 ± 173 N and a mean patellar tendon force of 869 ± 181 N, predicted by the finite element model. The mean ratio between the patellar tendon force and the quadriceps force was 0.74 ± 0.11.

Comparison of Contact Areas

Contact areas estimated by the model were within 5% of the contact areas measured from the weight-bearing MRI for 10 of the 16 subjects. Four of the 16 models displayed contact areas that differed from the experimental value by greater than 10%, with a maximum error in one subject of 32%. The shape of the contact areas were qualitatively similar to those measured from the MRI (Fig. 2). The orientation of the patella at the end of the simulation was also compared to its position measured from the MR images. On average, the patella orientation during the simulation was within 3.7 ± 5.9° of tilt and 4.7 ± 7.6° of rotation of the measured orientation.

Patellofemoral Cartilage Stresses in the Neutral Pose

Large variations in hydrostatic pressure and octahedral shear stress in the patellofemoral cartilage were found across the 16 subjects (Neutral orientation, Table 1). Mean stresses varied less than peak stresses; the greatest standard deviations occurring in the peak

hydrostatic pressure and peak shear stress in the patellar cartilage. Mean and peak hydrostatic pressures in the femoral cartilage were, on average, ~15–20% higher than hydrostatic pressures in the patella ($p < 0.001$). Conversely, the mean and peak octahedral shear stresses at the layer of cartilage closest to the bone were significantly less in the femoral cartilage compared to the patellar cartilage ($p < 0.001$).

Hydrostatic pressures within the cartilage were highest under the region of contact, correlating to regions with high contact pressure. The magnitude of hydrostatic pressure reduced only slightly through the depth of the cartilage. Octahedral shear stresses showed greater variation through the thickness of cartilage and did not necessarily correspond to regions of high contact pressure.

Effect of Femoral Rotation

The relative change in stress with femoral rotation was typically consistent within the same subject for the same condition. That is, if hydrostatic pressure in the femoral cartilage increased with femoral internal rotation, then octahedral shear stress in the femoral cartilage also increased with femoral internal rotation. Similarly, if shear stress in the patellar cartilage increased, then hydrostatic pressure within the patellar cartilage most likely increased under the same condition. Changes in the contact area at the joint in each simulation were also associated with changes in the stress state of the cartilage in each condition. This is illustrated in Figure 3, which shows the change in contact area of one subject from external femoral rotation, where contact was primarily on the medial facet of the trochlear groove (Fig. 3a) to internal rotation, where contact was mostly on the lateral facet of the trochlea (Fig. 3b). Peak cartilage stresses also shifted between the medial and lateral facets of the trochlear groove with external and internal rotation of the femur, respectively. This shift in stress distribution was consistent across subjects.

Table 1 summarizes the change in mean and peak cartilage stress variables with femoral internal and external rotation compared to the neutral orientation.

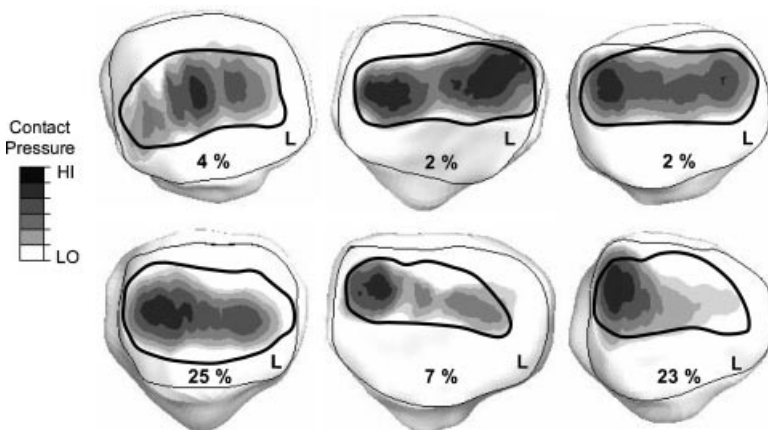


Figure 2. Example distributions of contact pressure on the surface of the patellar cartilage for six subjects in the neutral femur position. On each figure, a projected outline illustrates the contact area that is measured from the weight-bearing MRI. The percentage difference between the simulated contact area and the measured is also given (L = lateral).

Table 1. Mean and Peak Stresses within the Layer of Cartilage Closest to the Bone Boundary of the Patella and Femur for All Seven Simulation Conditions

			Internal Rotation [deg]				External Rotation [deg]			
			-15	-10	-5	Neutral	5	10	15	
Patella	Shear Stress	mean [SD]	1.2 [0.4]	1.2 [0.4]	1.2 [0.4]	1.2 [0.4]	1.2 [0.4]	1.2 [0.4]	1.2 [0.4]	
		peak [SD]	4.2 [2.0]	4.3 [2.1]	4.6 [2.4]	5.1 [3.0]	5.1 [2.7]	5.3 [3.1]	5.9 [3.6]	
	Hydrostatic Pressure	mean [SD]	1.3 [0.3]	1.3 [0.4]	1.3 [0.4]	1.3 [0.4]	1.2 [0.3]	1.2 [0.4]	1.2 [0.4]	
		peak [SD]	4.3 [1.5]	4.3 [1.6]	4.5 [2.0]	4.8 [2.5]	4.5 [2.0]	4.7 [2.4]	5.2 [2.9]	
Femur	Shear Stress	mean [SD]	0.8 [0.2]	0.8 [0.2]	0.8 [0.2]	0.9 [0.2]	0.8 [0.2]	0.9 [0.2]	0.9 [0.3]	
		peak [SD]	2.8 [0.7]	2.8 [0.8]	2.8 [0.8]	2.9 [0.8]	3.0 [0.8]	3.1 [0.9]	3.3 [0.9]	
	Hydrostatic Pressure	mean [SD]	1.5 [0.4]	1.5 [0.4]	1.5 [0.4]	1.5 [0.4]	1.4 [0.4]	1.4 [0.4]	1.4 [0.4]	
		peak [SD]	5.4 [1.7]	5.4 [1.7]	5.4 [1.9]	5.5 [2.0]	5.4 [2.0]	5.6 [2.2]	5.9 [2.3]	

Values presented are means across all subjects, with units of MPa. (SD: standard deviations).

Due to large variation in cartilage stress responses, the repeated measures analysis of variance did not detect any significant influence of rotation on stress level. Inspection of individual stress responses showed that some subjects experienced increased stress with femoral rotation, whereas other subjects experienced reduced stress under the same condition. Further analysis therefore focused on whether the femur or patellar cartilage stress variables increased by more than 10%, decreased by more than 10%, or remained the same with femoral rotation of $\pm 15^\circ$.

Internal rotation of the femur did not have a large effect on the *average* stress variables in the patellofemoral cartilage. Only 3 of the 16 subjects showed greater than 10% change in average stress with a 15° rotation. However, *peak* stress variables (both hydrostatic pressure and octahedral shear stress) were more susceptible to changes in femoral rotation. Approximately one-third of the subjects had increased peak femoral cartilage stress with femoral internal rotation. Another third of the subjects showed decreased peak hydrostatic and shear stress in the femoral cartilage with femoral internal rotation, and the last third had no change in peak stresses with femoral internal rotation. Thirty-five percent of the subjects had an increase in hydrostatic and shear stress in the patellar cartilage with internal rotation of the femur. Almost half of the subjects had a decrease in peak patellar cartilage stresses with femoral internal rotation, and 18% of the subjects did not have

any substantial change in peak patellar cartilage stress with femoral rotation.

External rotation of the femur had more of an effect on the peak stress variables than internal rotation. Peak patellar shear stresses increased in 75% of the subjects with 15° of femoral external rotation, and two-thirds of the subjects also had increased peak patellar hydrostatic pressure and peak shear stress in the femoral cartilage as a result of external rotation of the femur. A little over half of the subjects had increased peak hydrostatic pressure in the femoral cartilage with femoral external rotation. Interestingly, only one subject showed $>10\%$ reduction in peak stress variables with femoral external rotation to 15° . There was substantial anatomical variation between subjects as well as the variation in stress responses to internal and external femoral rotation (Fig. 4). None of the subjects showed a reduction in hydrostatic pressure with femoral external rotation, with five subjects increasing mean and peak cartilage stresses in both the femur and the patella compared to the neutral position.

Comparisons of Stress Variables with Contact Area

A power curve was found to provide the closest approximation (i.e., highest R^2 values) of the stress variables using the joint contact area predicted by the simulations. As expected, stresses within the cartilage increased rapidly with a reduction in contact area. Approximately 60% of the variation in mean hydrostatic

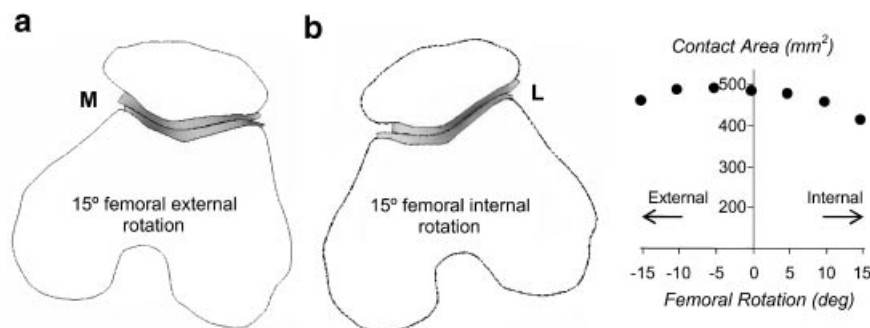


Figure 3. Effect of femoral internal and external rotation on patella orientation with respect to the femur. Axial images through a right knee of one subject illustrate the deviation of the patella with respect to the femur with femoral rotations up to 15° . Note how the patellar cartilage changes contact with the femur, moving to the medial facet (M) during femoral external rotation (a) and the lateral facet (L) during femoral internal rotation (b). The deviations in patellar orientation affect the patellofemoral contact area, shown on the right.

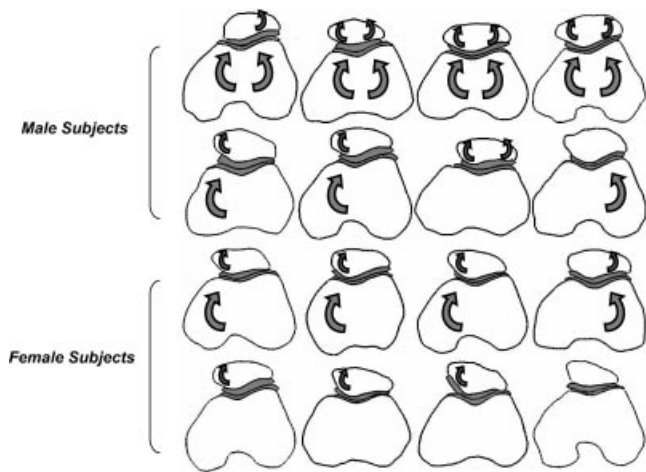


Figure 4. Variation in patellofemoral geometry and cartilage stress responses across all subjects with 15° internal and external rotation of the femur. Axial slice through midsection of the patella during a static squat to 60° of knee flexion. Arrows indicate if peak cartilage shear stress in the patella (small arrow) or femur (large arrow) are increased with changes in femoral internal (left curving arrow) or external rotation (right curving arrow). No arrow means that cartilage stress did not change or was reduced with femoral rotation. For illustrative purposes, all these models are presented as a right knee.

pressure within the patellar cartilage was accounted for by changes in contact area. Peak hydrostatic pressures in the patellar cartilage also correlated with the contact area from the simulation ($R^2 = 0.68$). However, mean and peak octahedral shear stresses in the patellar cartilage correlated less to contact area than hydrostatic pressures, with R^2 values of 0.31 and 0.53, respectively. Contact area was not as good a predictor of the stress within the femoral cartilage, compared to the patellar cartilage. The stress variable best predicted by contact area in the femoral cartilage was peak hydrostatic pressure ($R^2 = 0.43$), whereas contact area could only account for 30 and 26% of the variation in mean and peak shear stresses in the femoral cartilage, respectively.

The simple calculation of net joint stress (using net joint reaction force/measured contact area) accounted for 76% of the variation in mean hydrostatic pressures estimated in the patellar cartilage (Fig. 5a). This simplified stress calculation did not correlate as well to the average shear stresses in the patellar cartilage (Fig. 5b; $R^2 = 0.63$), nor did it correlate well to peak stress values ($R^2 = 0.41$ and 0.46 for hydrostatic pressure and shear stress; Fig. 5c and d, respectively).

DISCUSSION

The purpose of this study was to determine the influence of internal and external rotation of the femur on the stresses within the cartilage of the patellofemoral joint. It was hypothesized that hydrostatic pressure and octahedral shear stresses within the cartilage of the patella and femur would increase with internal rotation of the femur. This hypothesis was supported by only one-third of the subjects, who displayed an increase of more than 10% in both femoral and patellar cartilage

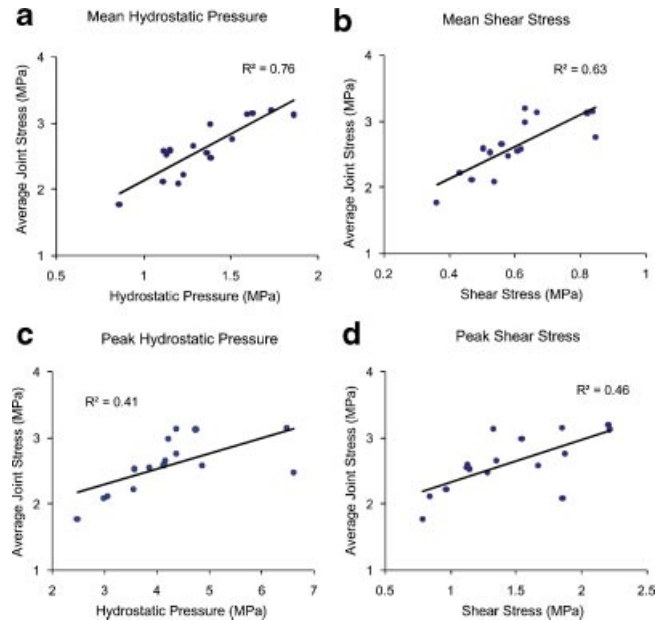


Figure 5. Correlations between simple measures of joint stress (net joint reaction force/measured contact area) and stresses estimated in the patellar cartilage by the finite element method. Mean hydrostatic pressure in the patella (a) was predicted better with the simple model than mean octahedral shear stress (b). Predictions of peak stress values were lower than predictions of mean stress values (c and d). Only simulations for the neutral pose were used for these comparisons, as contact areas were not measured from MRI in other postures.

stress with 15° internal rotation of the femur. Increased cartilage stress with internal rotation of the femur supports the clinical notion of “overloading” or “compression” of the lateral facet of the trochlea, which one might expect due to rotation of the femur or lateral displacement and tilt of the patella. However, in a similar number of subjects, femoral internal rotation had little effect on stresses within the cartilage, and in the other third of the subjects stress variables decreased with femoral internal rotation, contrary to our hypothesis. We also hypothesized that patellofemoral cartilage stress would decrease with femoral external rotation, yet the results from these simulations suggest that cartilage stresses in the patella and femur are more likely to increase with external rotation of the femur.

An important finding from this study is that cartilage stresses are not intuitively predicted based upon joint kinematics alone, which may seem to contradict conventional wisdom relating to patellofemoral biomechanics. The hydrostatic and octahedral shear stresses developed throughout the cartilage of the patellofemoral joint are a result of complex interactions between the articulating geometry of the patella and femur, cartilage morphology, cartilage material properties, and the distribution of forces acting on the patella. Variations in each of these parameters may be responsible for the different stress responses that resulted from these simulations. The fact that cartilage stresses increased with femoral rotation in some subjects but decreased in others might also suggest that the initial “neutral” orientation of the tibiofemoral

joint (taken from the weight-bearing MRI) may have covered a wide range of femoral internal and external rotation. These complex interactions also explain why simple measures of joint morphology (e.g., sulcus angle, patellar tilt, Q-angle, cartilage thickness), muscle strength (e.g., ratio of medial and lateral vasti activation, hip internal/external range of motion), or joint loading (e.g., knee joint moments) do not adequately reflect the stress state of the tissue, or predict the tissue response to various interventions. Nonlinear changes in stress variables and low correlations with contact area also suggest that simplified estimations of joint contact pressure cannot represent the stress state of the cartilage. This is particularly the case for peak shear stresses, which may be an important stress variant for understanding cartilage mechanobiology and pathology.²⁰ Li et al.¹¹ also concluded that it is difficult to explain cartilage stress distributions using contact pressures alone, even if the contact pressures are measured experimentally. Indeed, by only calculating contact pressures one might entirely overlook the fact that stresses within the femoral cartilage are different to those throughout the patellar cartilage. Although material properties were consistent for all of our simulations, it is known that shear stress and hydrostatic pressure are more sensitive to variations in material properties compared to surface pressures.¹¹ These findings highlight the need to develop and use finite element models with subject-specific loads, material properties, and kinematics to investigate patellofemoral joint cartilage stress distributions in both normal and pathological populations.

In general, cartilage stresses were more sensitive to external rotation of the femur, compared with internal rotation, with three-quarters of subjects having greater than 10% increase in peak shear stresses in the patellar cartilage with 15° of femoral external rotation. We hypothesized that the cartilage in the patellofemoral joint might experience a reduction in stress with femoral external rotation, although it became clear that the reduction in contact area as the patella moved from the lateral side of the trochlea to the relatively smaller medial side of the trochlear groove, caused an increase in both femoral and patellar cartilage stress. Changes in cartilage thickness could also play a role in this change in stress. Lee and colleagues⁸ measured contact pressures in cadavers with external rotation of the femur and showed that 30° of external rotation of the femur resulted in a greater increase in pressure (~30%) compared to internal rotation of the femur (~25% increase). Such extreme ranges of femoral rotation might occur in patients with rotational deformities; however, it is difficult to determine if such orientations exist in a healthy population without being able to accurately measure patellofemoral kinematics. Furthermore, passive soft tissue structures, such as the medial and lateral patellofemoral ligaments and peripatellar retinaculum were not modeled in these simulations but are likely to assist in maintaining contact area at extreme ranges of motion. As with internal rotation of the femur, a number

of individuals remained insensitive to changes in femoral external rotation, and in contrast with our hypothesis, there was not a significant reduction in peak stress in the patellar or femoral cartilage with external rotation.

It is generally agreed that hydrostatic pressures are beneficial for the maintenance of healthy cartilage, whereas shear stresses are associated with degeneration of cartilage.¹² One might therefore expect that the increased shear stresses experienced by the patellar cartilage are more likely to result in cartilage damage or deterioration. This is supported by clinical findings, where the most common site for grade III lesions of articular cartilage (defined as deep fissuring without exposed bone) occur in the patella³² and not the trochlea. Higher shear stresses in the patellar cartilage may also be responsible for exciting nociceptors, which are known to exist in the subchondral bone plate of the patella.³³ Patellar cartilage was also more sensitive to femoral rotation compared to femoral cartilage, with a greater number of subjects showing increased peak shear stresses with rotations of 15°. The caveat here is that all of the subjects who participated in this study were pain free and had no known degenerative adaptation or joint pathology. Pathological joints may display different trends in cartilage stresses.

Several limitations of these simulations should also be discussed in light of the current findings. For the purpose of investigating the isolated effect of femoral internal and external rotations on cartilage stresses in the femur and patella, the rotations applied to the femur during these simulations were not coupled to any motion of the tibia. In an intact joint, the muscles, ligaments, patellar tendon, and joint capsule provide a mechanical coupling between the femur and the tibia such that rotations of the femur might also influence the orientation of the tibia (and vice versa). These simulations therefore offer an estimate of the effect of femoral rotation on cartilage stresses, but may not reflect the exact orientation of the tibiofemoral joint in subjects who move to these ranges of internal and external rotation.

The quadriceps muscles in these simulations were modeled as simple line segment actuators whose initial line of action was determined from the weight-bearing MR images. During the internal and external femoral rotation simulations, the origin of the quadriceps did not change with the change in orientation of the femur. In vivo it is not known to what effect femoral internal and external rotation has on the effective line of action of the quadriceps. Modeling the complete quadriceps muscles as three-dimensional deformable elements and including the orientation of the muscle fiber directions could account for the relationship between the muscles line of action and the orientation of the femur.

Four of the simulations did not closely match the contact area measured in the weight-bearing MRI (>10%). This may be due to poor estimates of the muscle force distribution, which might explain the two lower right cases in Figure 2, or discrepancies in the material properties, which would explain the lower left case in

Figure 2. For the purpose of this study, we did not attempt to correct for these; however, one might envision an optimization/calibration scheme to alter the muscle force distribution and/or material properties to match experimental data over a wide range of conditions to improve the model predictions.

In this study, we chose to model cartilage as a linear elastic material. Although such a material model cannot account for time-dependent changes in stress or deformation, a linear elastic model for cartilage has been advocated for and used by a number of previous investigators.^{7,11,12,25,26} and is considered reasonable and appropriate when simulating activities with loading frequencies of 0.01 Hz and higher. For the purposes of investigating the effect of changing the orientation of the tibiofemoral joint, this simplification seems reasonable.

This study provides a description of the hydrostatic pressure and octahedral shear stress distribution in the cartilage of the patellofemoral joint and how these stresses can be influenced by internal and external rotations of the femur. There is increasing interest in the clinical community as to the influence of femoral rotation on the development and treatment of patellofemoral pain. Cartilage stresses within the femoral and patellar cartilage can indeed be influenced by femoral rotation; however, the magnitude and direction of this change is subject-specific and not intuitively determined. Some individuals respond to femoral internal rotation with large changes in cartilage stresses, whereas others show little or no change with the same degree of femoral rotation. This insight has clinical relevance, particularly when considering treatment strategies to reduce stress. Assuming that cartilage stresses are related to pain from increased stresses transmitted through the cartilage into the subchondral bone, individuals who are more sensitive to changes in femoral rotation might respond positively to therapies or intervention strategies that focus on controlling femoral rotation. However, subjects who are relatively insensitive to changes in femoral rotation may not respond to any intervention that is designed to alter femoral rotation, such as stretching and strengthening of hip muscles. The use of finite element models with subject-specific loads and boundary conditions provides a powerful framework to identify important variables that relate to potential changes in tissue-level stresses and how these stresses might relate to potential joint and cartilage pathology.

ACKNOWLEDGMENTS

Financial support for this study was from the Department of Veterans Affairs, Rehabilitation R&D Service (grant # A2592R), the National Institute of Health (1R01-EB005790, U54 GM072970, U54 GM072970, HD33929, and HD046814), and Stanford Regenerative Medicine (1R-90DK071508).

REFERENCES

- Shelburne KB, Torry MR, Pandy MG. 2005. Muscle, ligament, and joint-contact forces at the knee during walking. *Med Sci Sports Exerc* 37:1948–1956.
- Brechtner JH, Powers CM. 2002. Patellofemoral joint stress during stair ascent and descent in persons with and without patellofemoral pain. *Gait Posture* 16:115–123.
- Costigan PA, Deluzio KJ, Wyss UP. 2002. Knee and hip kinetics during normal stair climbing. *Gait Posture* 16:31–37.
- Scott SH, Winter DA. 1990. Internal forces of chronic running injury sites. *Med Sci Sports Exerc* 22:357–369.
- Fulkerson JP, Shea KP. 1990. Mechanical basis for patellofemoral pain and cartilage breakdown. In: Ewing JW, editor. *Articular cartilage and knee joint function: basic science and arthroscopy*. New York: Raven Press; p 93–101.
- Heino Brechtner J, Powers CM. 2002. Patellofemoral stress during walking in persons with and without patellofemoral pain. *Med Sci Sports Exerc* 34:1582–1593.
- Cohen ZA, Henry JH, McCarthy DM, et al. 2003. Computer simulations of patellofemoral joint surgery. Patient-specific models for tuberosity transfer. *Am J Sports Med* 31: 87–98.
- Lee TQ, Anzel SH, Bennett KA, et al. 1994. The influence of fixed rotational deformities of the femur on the patellofemoral contact pressures in human cadaver knees. *Clin Orthop Relat Res* 302:69–74.
- Lee TQ, Morris G, Csintalan RP. 2003. The influence of tibial and femoral rotation on patellofemoral contact area and pressure. *J Orthop Sports Phys Ther* 33:686–693.
- Lee TQ, Yang BY, Sandusky MD, et al. 2001. The effects of tibial rotation on the patellofemoral joint: assessment of the changes in in situ strain in the peripatellar retinaculum and the patellofemoral contact pressures and areas. *J Rehabil Res Dev* 38:463–469.
- Li G, Lopez O, Rubash H. 2001. Variability of a three-dimensional finite element model constructed using magnetic resonance images of a knee for joint contact stress analysis. *J Biomech Eng* 123:341–346.
- Carter DR, Beaupré GS. 2001. *Skeletal function and form—mechanobiology of skeletal development, aging, and regeneration*. New York: Cambridge University Press p 201–234.
- Benoit DL, Ramsey DK, Lamontagne M, et al. 2006. Effect of skin movement artifact on knee kinematics during gait and cutting motions measured in vivo. *Gait Posture* 24:155–164.
- Lafortune MA, Cavanagh PR, Sommer HJ, et al. 1992. Three-dimensional kinematics of the human knee during walking. *J Biomech* 25:347–357.
- Asano T, Akagi M, Koike K, et al. 2003. In vivo three-dimensional patellar tracking of the femur. *Clin Orthop Relat Res* 413:222–232.
- Powers CM, Ward SR, Fredericson M, et al. 2003. Patellofemoral kinematics during weight-bearing and non-weight-bearing knee extension in persons with lateral subluxation of the patella: a preliminary study. *J Orthop Sports Phys Ther* 33:677–685.
- Ireland M, Willson J, Ballantyne B, et al. 2003. Hip strength in females with and without patellofemoral pain. *J Orthop Sports Phys Ther* 33:671–676.
- Mascal CL, Landel R, Powers C. 2003. Management of patellofemoral pain targeting hip, pelvis, and trunk muscle function: 2 case reports. *J Orthop Sports Phys Ther* 33: 647–660.
- Powers CM. 2003. The influence of altered lower-extremity kinematics on patellofemoral joint dysfunction: a theoretical perspective. *J Orthop Sports Phys Ther* 33:639–646.
- Beaupré GS, Stevens SS, Carter DR. 2000. Mechanobiology in the development, maintenance, and degeneration of articular cartilage. *J Rehabil Res Dev* 37:145–151.
- Besier TF, Gold GE, Beaupré GS, et al. 2005. A modeling framework to estimate patellofemoral joint cartilage stress in vivo. *Med Sci Sports Exerc* 37:1924–1930.

22. Besier TF, Draper CE, Gold GE, et al. 2005. Patellofemoral joint contact area increases with knee flexion and weight-bearing. *J Orthop Res* 23:345–350.
23. Gold GE, Besier TF, Draper CE, et al. 2004. Weight-bearing MRI of patellofemoral joint cartilage contact area. *J Magn Reson Imaging* 20:526–530.
24. Donahue TL, Hull ML, Rashid MM, et al. 2002. A finite element model of the human knee joint for the study of tibiofemoral contact. *J Biomech Eng* 124:273–280.
25. Higginson GR, Snaith JE. 1979. The mechanical stiffness of articular cartilage in confined oscillating compression. *Eng Med* 8:11–14.
26. Beaupré GS, Carter DR. 1992. Finite element analysis in biomechanics. In: Biewener AA, editor. *Mechanics; structures and systems; a practical approach*. New York: Oxford University Press; p 149–174.
27. Ateshian GA, Hung CT. 2005. Patellofemoral joint biomechanics and tissue engineering. *Clin Orthop Relat Res* 81: 81–90.
28. DeFrate LE, Wook Nah K, Papannagari R, et al. 2007. The biomechanical function of the patellar tendon during in-vivo weight-bearing flexion. *J Biomech* 40: 1716–1722.
29. Reeves ND, Maganaris CN, Narici MV. 2003. Effect of strength training on human patella tendon mechanical properties of older individuals. *J Physiol* 548:971–981.
30. Lloyd DG, Besier TF. 2003. An EMG-driven musculoskeletal model to estimate muscle forces and knee joint moments in vivo. *J Biomech* 36:765–776.
31. Farahmand F, Senavongse W, Amis AA. 1998. Quantitative study of the quadriceps muscles and trochlear groove geometry related to instability of the patellofemoral joint. *J Orthop Res* 16:136–143.
32. Curl WW, Krome J, Gordon ES, et al. 1997. Cartilage injuries: a review of 31, 516 knee arthroscopies. *Arthroscopy* 13:456–460.
33. Wojtys EM, Beaman DN, Glover RA, et al. 1990. Innervation of the human knee joint by substance-P fibers. *Arthroscopy* 6:254–263.